Applied Surface Science 341 (2015) 109–119

Contents lists available at ScienceDirect

Applied Surface Science

journal homepage: www.elsevier.com/locate/apsusc

Electrophoretic deposition of multi-walled carbon nanotubes on porous anodic aluminum oxide using ionic liquid as a dispersing agent

F. Hekmat [a], B. Sohrabi [a,*], M.S. Rahmanifar [b], A. Jalali [a]

[a] Department of Chemistry, Surface Chemistry Research Laboratory, Iran University of Science and Technology, P.O. Box 16846-13114, Tehran, Iran
[b] Faculty of Basic Science, Shahed University, Tehran, Iran

ARTICLE INFO

Article history:
Received 16 August 2014
Received in revised form
29 December 2014
Accepted 20 February 2015
Available online 28 February 2015

Keywords:
Vertically-aligned carbon nanotubes
Electrophoretic deposition
Anodic aluminum oxide
Ionic liquid
Electrochemical double layer capacitor

ABSTRACT

Multi-wall carbon nanotubes (MW-CNTs) have been arranged in nanochannels of anodic aluminum oxide template (AAO) by electrophoretic deposition (EPD) to make a vertically-aligned carbon nanotube (VA-CNT) based electrode. Well ordered AAO templates were prepared by a two-step anodizing process by applying a constant voltage of 45 V in oxalic acid solution. The stabilized CNTs in a water-soluble room temperature ionic liquid (1-methyl-3-octadecylimidazolium bromide), were deposited in the pores of AAO templates which were conductive by deposition of Ni nanoparticles in the bottom of pores. In order to obtain ideal results, different EPD parameters, such as concentration of MWCNTs and ionic liquid on stability of MWCNT suspensions, deposition time and voltage which are applied in EPD process and also optimal conditions for anodizing of template were investigated. The capacitive performance of prepared electrodes was analyzed by measuring the specific capacitance from cyclic voltammograms and the charge–discharge curves. A maximum value of 50 Fg^{-1} at the scan rate of 20 mV s^{-1} was achieved for the specific capacitance.

© 2015 Elsevier B.V. All rights reserved.

1. Introduction

Ever since their discovery by Iijima in 1991 [1], carbon nanotubes (CNTs) are a novel generation of materials which widely used to make a variety of advanced nanostructures, including electron field emission devices [2,3], storage of hydrogen [4,5], batteries [6], supercapacitors [7,8], electrochemical sensors [9], and electromechanical actuators [10], because of their unique electrical, optical, and mechanical properties, such as superior mechanical strength, metal-like electrical conductivity, and extreme aspect ratios [11]. Supercapacitors or Electrochemical double layer capacitors (EDLCs) are electrochemical energy storage devices that can provide a large amount of electrical energy in a short period of time [12]. Because the EDLCs store charges in the electric double layer formed at the electrode/electrolyte interface, maximizing the amount of surface area of electrodes play an important role in supercapacitors [13]. Recent researches demonstrated the improved rate capability for aligned CNTs over randomly entangled CNTs, so many researchers have tried to develop methods to control and align CNTs in desire direction [14–16].

Two classes of alignment techniques can be distinguished: one attempt growing the tubes along a given direction, either within the substrate or normal bundles [14]. Among the many kind of CNT synthesis methods, chemical vapor deposition (CVD), especially plasma enhanced chemical vapor deposition which is called PECVD, is effective for VA-CNT volume production [17]. In another method which is known as post-growth method, a purification and an effective dispersion of CNTs in a suitable solvent by aid of a disparent (surfactants or polymers) is required to obtain a homogenous well dispersed CNT suspension, which is play a key role in controlling manipulation of CNTs [14,18]. Several interesting approaches have been developed to align CNTs after their synthesized. Jin et al. reported the alignment of CNTs by stretching of polymer/CNT film [19]. Bendiab and co-workers used a uniaxial pressure (~10 kbars) to align CNTs [20]. By the doctor blade technique, the embedded CNTs in polymer film, warmed to be soft and then rubbed with a blade in a desire direction to induce the elastic force which can align CNTs [14]. Bulk acoustic waves (BAWs) are used to align MWCNTs in polymer composite materials by Haslam and Raeymaekers [21]. It is noticeable that in all of these methods, CNTs are highly surrounded by a polymer network and thus CNTs will not be able to express all of their unique properties. During the filtration method, dispersed CNTs crossing through a micropore filter to prepare aligned CNTs [22]. Along fiber drawing or spinning method, CNTs forced to be aligned within the fibers due

* Corresponding author. Tel.: +98 77240540x6275.
E-mail address: sohrabi_b@iust.ac.ir (B. Sohrabi).

http://dx.doi.org/10.1016/j.apsusc.2015.02.142
0169-4332/© 2015 Elsevier B.V. All rights reserved.

to the combination of shear forces and the liquid crystalline phase [21,23]. Lungmuir–Blodgett (LB) technique is gently done by sinking a template into a CNTs suspension and pulling it out slowly to produce a thin and homogenous layer of CNTs on template [14]. Success of these methods tightly depends on precision in speed, direction and intensity of applied mechanical force. Among many methods have been reported for controlling alignment of CNTs, applying an external magnetic or/and electric field were widely used for various applications. Unlike other methods, these two last mentioned methods caused minimum structural damage without considerable changes in characteristic properties of CNTs. By using a powerful magnetic field (>7 T) a well dispersed CNT suspension is develop on substrate. Despite the efficiency of this method, its disadvantage is costs and preparation of a strong magnetic field [14]. The last method which is called EPD, allows controlling of thickness and shape of deposited film by using an electric field [17]. However, there are a variety of post-growth methods to align CNTs, but the success of EPD is to the fact that it is fast, cost effective technique usually requiring simple equipment [24].

Because of the strong van der Waals interaction between tubes, CNTs have extremely poor solubility in most of solvents and it makes their characterization and processing difficult, which is the major limitation to their practical applications [25]. Specifically, CNTs exist as heavily entangled aggregates of bundles [26,27] containing hundreds of closely packed CNTs [26].

Recently room temperature ionic liquids (RT-ILs), with unique physicochemical properties such as wide liquid temperature range, high thermal stability, negligible vapor pressure, non-flammability, increased electrochemical window, and relatively high ionic conductivity have been widely applied as excellent green reaction media [28,29]. Modification of CNTs with ILs is expected to improve their compatibility and stability [30]. Nowadays dispersing CNTs with ILs seems to become an interesting topic and attracted much attention, so some studies have been done in this field. Imidazolium based ILs, such as 1-butyl-3-methylimidazolium tetra fluoro borate triggered single walled carbon nanotubes (SWCNTs) to form gel called "Bucky gel" [29]. Kocharova et al. demonstrated that CNTs could be stably dispersed in water with aid of small amount of 1-dodecyl-3-methylimidazolium bromide [31]. Crescenzo and co-workers indicated that 1-hexadecyl-3-vinyl-imidazolium bromide is a good agent to dispersing SWCNTs [31]. Liu et al. found that ionic-liquid-type Gemini imidazolium surfactant ([C_n-C_4-C_n im] Br_2, n = 12, 14) can effectively disperse MWCNTs even at very low concentration [32]. Gao and co-workers discussed that electrostatic repulsion, hydrophobic interactions, cation–π, and n–π interactions played important roles in dispersion of MWCNTs by Poly (1-glycidyl-3-methylimidazolium chloride) (PGMIC) [33]. Lu et al. reported that MWCNTs can be effectively dispersed in aqueous solution by alkyl-triphenyl phosphonium bromide (C_nTPB, n = 12 and 14) [25]. Despite many researches were carried out, there are still significant challenges to obtain well-separated CNTs with aid of room temperature ionic liquids to achieve dense array of vertically aligned carbon nanotubes (VA-CNTs) in post growth aligning methods. In this work, we used a small amount of 1-methyl-3-octadecylimidazolium bromide to disperse MWCNTs in aqueous solution. As already mentioned, the homogeneous distribution of CNTs within a suspension plays a key role in inflicting many important properties during the post-growth methods for aligning CNTs. In recent years, various techniques were suggested to obtain a quantitative assessment for exfoliated CNTs concentration in suspensions. In compare with common methods such as Raman spectroscopy and atomic force microscopy (AFM) which possess a good ability on determination of dispersion quality and exfoliation state, but these cannot give any quantitative information on exfoliated CNT concentration [34]. The UV–vis approach is a simple and effective method for calculating the concentration of surfactant-dispersed CNTs in solution [34–37]. In this study, we followed a method proposed by Liu et al. [35] for quantifying dispersion of CNTs which is based on a simple ultracentrifuge process.

After dispersing CNTs by this long chain IL, well dispersed CNTs are aligned on desired template by applying electric field. EPD is achieved via the motion of charged CNTs dispersed in IL, toward a conducting electrode under an applied electric field. The final goal is production of a film where most CNTs are aligned to certain direction [14].

Electrophoretic motion of charged dispersed CNTs during EPD results in the accumulation of CNTs, which are encapsulate within an IL micelle and formation of homogenous and rigid deposit at the relevant electrode [17,24]. In this study we used a periodic porous anodic aluminum oxide (AAO) electrode, which is being conductive substrate by electrochemical deposition of Ni nano particles as catalyst in the bottom of the nanoholes of AAO template to align individual dispersed CNTs. The structure of AAO template can be described as close-packed hexagonal arrays of parallel cylindrical nanoporous perpendicular to the surface on the top of the underlying Al substrate [38].

We report here a VA-CNT based electrode prepared by the EPD technique, which has the advantages of fast and simple formation. The electrodes built from such methods have exhibited acceptable electrochemical results, which indicate that this post-growth technique is an effective method in fabricating CNT electrodes for EDLCs and other similar devices.

2. Experimental

2.1. Chemicals

The ionic liquid was 1-methyl-3-octadecylimidazolium bromide ([C18C1im] Br) (>98%), which has been purchased from Kimia Exir (Iran) and used as received. The MWCNTs (length 0.1–10 μm, outer mean diameter 10–15 nm, mean number of walls 5–15), were supplied by Arkema Co. Ltd. (France). High-purity (99.9995%) 0.3 mm thickness, 30 mm width aluminum foil was purchased from Merck KGaA (Germany). Other solvents and reagents, except chromic anhydrate, obtained from Merck (Germany) and they used as received. Chromic anhydrate was purchased from KANTO Chemical Co., Inc. (Japan). Finally, doubly ionized water was obtained from an OES water purification system (USA).

2.2. Equipments

Carbon nanotubes were dispersed stably in water in presence of small amount of long chain IL by using a UP400S ultrasound processor from Hielscher Ultrasound GmbH (Teltow, Germany). Dispersed MWCNTs were characterized by UV–vis on a computer-controlled spectrophotometer (UV mini 1240, Shimadzu, Japan). The wavelength range from 200 to 800 nm was used to examine the absorbance of MWCNT suspensions. Before measurements, each sample was diluted by di-ionized water to the concentration of one-fifteenth of its initial concentration, and simultaneously the corresponding IL aqueous solution without CNTs was used as the bulk. The interactions between MWCNTs and ILs were studied by Infrared spectrometer (8400S, Shimadzu, Japan). The zeta potential measurements were done by using a Malvern Zeta Sizer 3000 HAS (Malvern instruments, UK), Because of the most necessary prerequisite for successful EPD is depends on preparation of a stable dispersion of CNTs, which have a high zeta potential [39].

DC power suppliers (MP6003, Megatek, Germany) were used in order to apply electric field in preparation of AAO template and also to deposition of dispersed CNTs during the EPD process. The morphology of the resultant AAO templates before and after

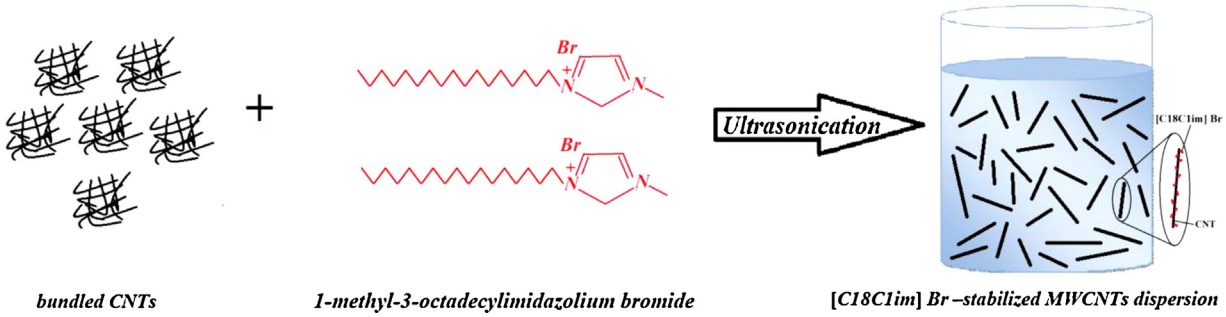

Fig. 1. Schematic procedures for production of IL stabilized-MWCNT suspension: (a) randomly entangled CNTs, (b) 1-methyl-3-octadecylimidazolium bromide, and (c) well dispersed MWCNTs in aqueous solution by [C18C1im]Br.

deposition of CNTs has been investigated by using of a scanning electron microscopy (TESCAN, VEGA, Czech Republic) and their EDX analysis were obtained with a scanning electron microscope (FE-SEM/EDX) (TESCAN, Mira II LMU, Czech Republic). Different electrochemical techniques were used to characterize the capacitive performance of as prepared electrodes. Cyclic voltammetry (CV) and charge–discharge galvanostatic experiments were conducted Electro analyzer system SAMA 500 (Iran) and Kimia stat (Iran), respectively. All of the electrochemical tests were carried out in 1.0 M Na_2SO_4 aqueous solution at room temperature in a three electrodes configuration using a saturated Ag/AgCl as the reference electrode and a graphite counter electrode.

2.3. Preparation of CNT suspension for EPD

The suspensions of MWCNTs were prepared by adding 4 mg MWCNTs into 10 ml of 1-methyl-3-octadecylimidazolium bromide aqueous solutions, and then the solutions were sonicated for 10 min by probe sonicator with a power density of 80 W cm^{-2}. In order to sedimentation of large tube bundles, the suspension of MWCNTs was stored at room temperature for 24 h, After one day, the resulting suspension were centrifuged for 10 min with 2000 rpm, in order to separate the precipitation from the bulk solutions. Fig. 1 schematically illustrates the dispersing process of CNTs by using small amount of [C18C1im] Br as disparent. To evaluate the quantitative characterization of CNTs dispersions, the suspension of MWCNTs in [C18C1im] Br aqueous solution (C_0) was prepared with the method which was mentioned above. Since the Beer-Lambert law is not obeyed in the strong absorption which is attributed to the high analyte concentration [34], a series of diluted samples with concentrations of $C_0/2$, $C_0/4$, $C_0/8$, $C_0/16$, $C_0/32$, and $C_0/64$ were prepared. Prepared samples were centrifuged for varied period of time (1, 2, 5, 10, 30, 60 min) with 14,000 rpm [35], then a UV–vis based method were used for the semiquantitative characterization of prepared CNT suspensions.

2.4. Preparation of AAO template

The AAO template is fabricated by using a two-step anodization process as shown in Fig. 2. First, a high-purity aluminum sheet with dimensions of 30 mm × 30 mm × 0.3 mm was degreased in acetone ultrasound and rinsed in an ethanol solution, followed by annealing at 500 °C for 5 h [40]. Before anodizing, the annealed sample was electropolished in a 1:4 volume mixture of perchloric acid (60 wt%) and ethanol (96 wt%) at 3 °C, and constant DC voltage of 20 V for 1 min were applied to obtain mirror finish. The two-step anodization was chosen to prepare an ordered porous AAO template. The first anodizing process was carried out under a constant voltage of 45 V dc in a 0.3 M oxalic acid solution at 5 °C for 20 h. The AAO film was chemically etched in a mixture of chromic acid (1.8 wt%) and phosphoric acid (6 wt%) at 75 °C for 3 h, then the second anodizing process was done for 1 h, under the same conditions as the first anodization process mentioned above, which resulted in formation of a highly ordered porous AAO template with a pore depth of about 2 μm [41,42]. In order to facilitate the uniform electrodeposition of Ni nanoparticles as catalyst, the voltage was dropped from 45 to 14 V at the rate of 0.5 V min^{-1}, which was done immediately at the end of the second anodization. Because the thickness of the barrier layer is proportional to applied voltage, the barrier layer was almost completely removed when the voltage reached 14 V [43,44].

After elimination of the barrier layer, the remaining Al substrate was removed in a saturated copper sulphate ($CuSO_4$) aqueous solution in chloridric acid (HCl) at room temperature [45]. Finally, the resulting AAO template was immersed in a 1.0 M aqueous phosphoric acid solution at room temperature for 40 min to eliminate the barrier layer on the bottom side, and simultaneously widen the pores [40]. One side of AAO membrane was sputtered with a layer of Au as a work electrode. The Ni catalyst was electrochemically deposited at the pore bottom of the AAO template in a three-electrode electrochemical system from an aqueous solution of 0.32 M $NiSO_4{\cdot}6H_2O$, 0.08 M $NiCl_2{\cdot}7H_2O$, and 0.28 M H_3BO_3, which is called Watt bath [45]. In order to have the better results in electro deposition of Ni catalysts in the bottom of pores, the pH value of the electrolyte was adjusted to about 2.0 with 0.1 M H_2SO_4 solution [45]. The electrochemical deposition of Ni catalyst was performed by using AAO template, which sputtered with a layer of Au as working electrode, platinum as counter electrode, and Ag/AgCl as reference electrode, and all of the potentials refer to the reference electrode.

2.5. Electrophoretic deposition of CNTs

As it shown in Fig. 3 the EPD was done in a two-electrode system, where resulting conductive AAO template by deposition of Ni catalyst, with exposed area of 1 cm × 1 cm were used as cathode, and Ni paper electrode with an exposed area of 2 cm × 2 cm were used as anode. These two electrodes were used in an electrophoretic deposition cell with an electrode gap of 7 mm. Care was taken that these two electrodes were parallel to each other. The DC electrophoretic deposition of VA-CNTs was conducted at 100 V for 1 min. After completing the deposition, the AAO membrane was dried under room temperature in desiccators for 24 h. Then prepared electrode placed at room temperature in NaOH etching solution to removing the AAO template partially and the resulting template immersed in dilute water immediately.

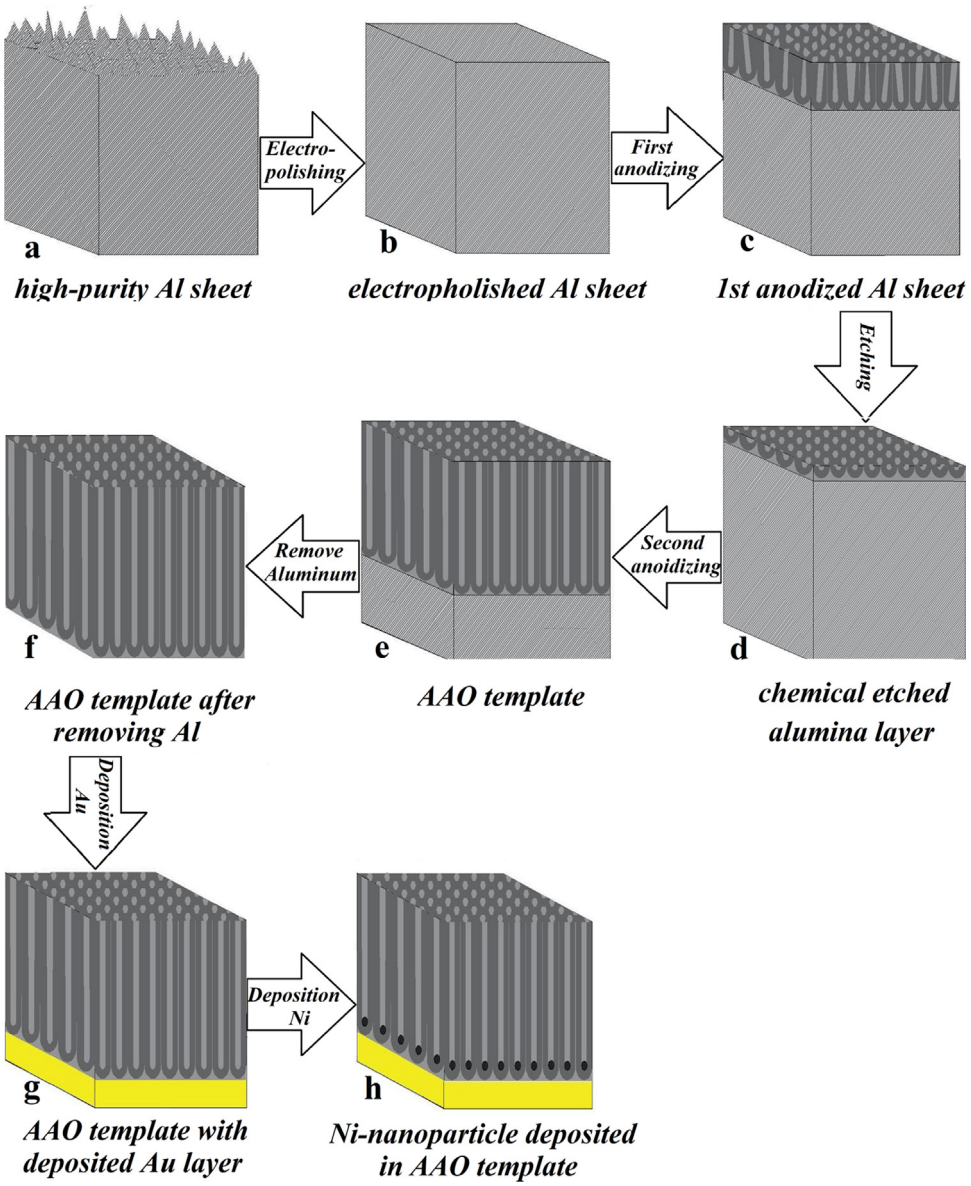

Fig. 2. Scheme of AAO process: (a) high purity aluminum sheet, (b) electropolished aluminum sheet, (c) First anodized aluminum sheet, (d) chemical etched alumina layer, (e) prepared AAO after a two-step anodization process, (f) AAO template after removing excess aluminum layer, (g) AAO template with deposited Au layer, and (h) resulting conductive AAO template by electrochemical deposition of Ni particles.

3. Results and discussion

3.1. Dispersion of MWCNTs by 1-methyl-3-octadecylimidazolium bromide Ionic Liquid

Fig. 4a shows the MWCNTs in aqueous solution before adding 1-methyl-3-octadecylimidazolium bromide ([C18C1im] Br). We noticed that even after 1hr of ultrasound, MWCNTs hardly agglomerate in aqueous solution. In contrast, after adding 1-methyl-3-octadecylimidazolium bromide into the same aqueous solution, a black homogenous dispersion was obtained, which could keep stable for more than 10 months. Because adding small amount of 1-methyl-3-octadecylimidazolium bromide into aqueous solution (only 0.4 mM in Fig. 4b) to disperse the MWCNTs, we can claim that 1-methyl-3-octadecyleimidazolium bromide is an excellent dispersant for dispersing CNTs.

In this work, we studied the effect of 1-methyl-3-octadecylimidazolium bromide concentration on dispersion of MWCNTs in aqueous solution. UV–vis is usually used to estimate the stability of dispersed CNTs, It has been reported that there is almost no absorption band in UV–vis region for bundled CNTs, however individual CNTs are active in this region and strong absorption can be observed [32]. Fig. 5a shows that 1-methyl-3-octadecylimidazolium bromide aqueous solutions display only negligible absorptions in the wavelength range from 200 to 800 nm, so the effect of ILs on the absorptions of MWCNT suspensions in UV–vis region can be ignored [32]. Fig. 5b shows that the MWCNT suspensions have strong UV–vis adsorption, and the maximum absorbance appeared around 260 nm, which is in agreement with previous reports [32].

On the other hand, because of the UV–vis region is scarcely activated by bundled CNTs, while it can be activated by individual CNTs, so with increasing of individual CNTs concentration in aqueous suspension, it can be expected that the absorbance of CNTs at the same wave length being increased [33]. According to these evidences, we can judge about the amount of individually dispersed

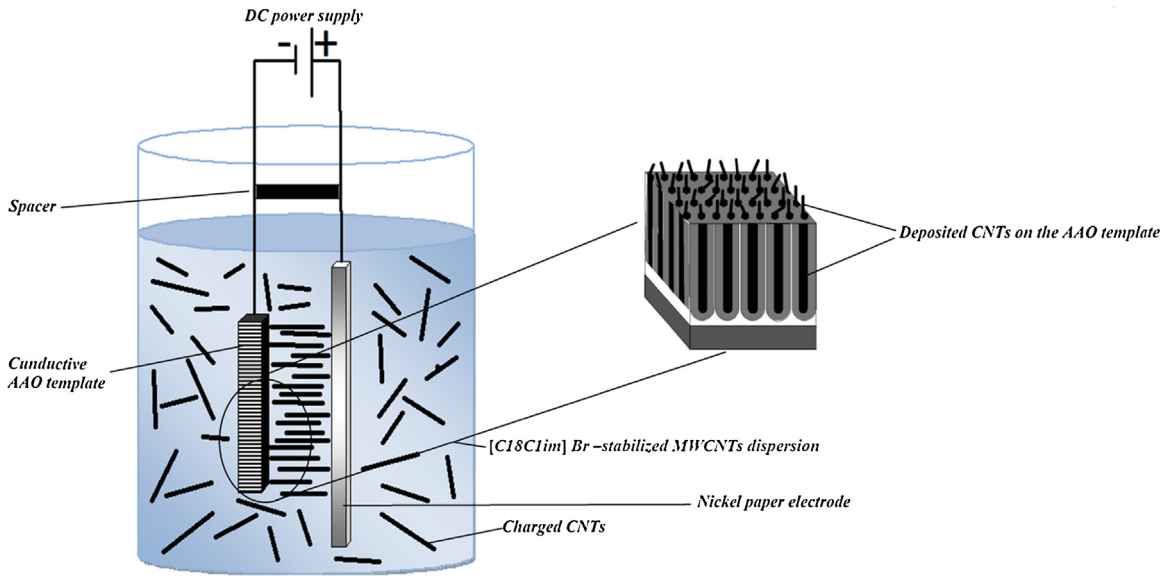

Fig. 3. Schematic diagram of an EPD cell for electrophoretic deposition of well dispersed CNTs on the cathode (as prepared AAO template).

CNTs based on the intensity of UV–vis absorption peaks, and we can determine the ability of different concentrations of 1-methyl-3-octadecylimidazolium bromide to disperse MWCNTs by UV–vis spectra.

Fig. 6a shows the absorbance of different concentrations of MWCNT suspensions, and in Fig. 6b shown that there is no linear relationship between the absorbance intensity of MWCNTs and IL concentration.

As it can be expected, the best concentration of 1-methyl-3-octadecylimidazolium bromide to disperse CNTs is around critical micelle concentration (CMC), so we investigated dispersion of CNTs by using [C18C1im] Br around CMC of ionic liquid, and the curves in Fig. 6, suggest that the best concentration of 1-methyl-3-octadecylimidazolium bromide to disperse 4 mg of MWCNTs was 0.4 mM.

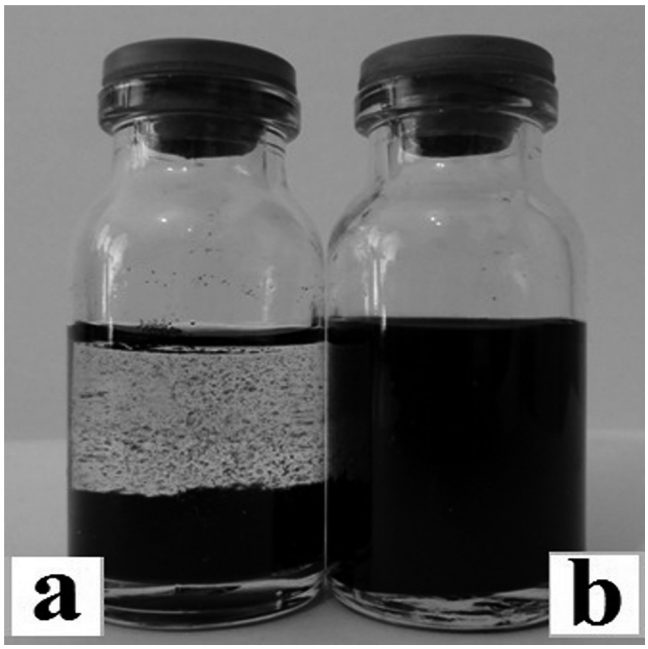

Fig. 4. Aqueous MWCNT dispersions: (a) without IL, imaged after 1 hr (b) with 0.4 mM of 1-methyl-3-octadecylimidazolium bromide, imaged after 10 months.

Semi-quantitative characterization of CNT dispersion was done by using a simple ultracentrifuge method for evaluating the stability of CNT suspensions [35]. Fig. 7a shows the UV–vis spectra of diluted 1-methyl-3-octadecylimidazolium bromide stabilized MWCNT dispersions (C_0/16, C_0/32, and C_0/64) which were centrifuged for different periods (0, 1, 2, 5, 10, 30, 60 min). As it can be seen in Fig. 7a, the absorbance of suspension which refers to the individual CNTs were decreased by decreasing the initial concentration and also decreased with increasing the centrifugation time [35]. Absorbance at two arbitrary wavelength (260 and 600 nm) was plotted versus their corresponding concentration values (the inset of Fig. 7a), which following the Lambert–Beer's law [35,46].

The absorbance diagrams of the series diluted [C18C1im] Br-stabilized MWCNT suspensions centrifuged for different periods of time at $\lambda = 600$ nm, $A(C_d, t)$, against their absorbance without centrifugation, $A(C_d, t = 0)$, at the same wavelength are linear (the inset of Fig. 7b). Liu et al. derive a logical relationship between the absorbance $A(C_d, t)$ and $A(C_d, t = 0)$ as follows:

$$A(C_d, t) = F(t)A(C_d, t = 0) \quad (1)$$

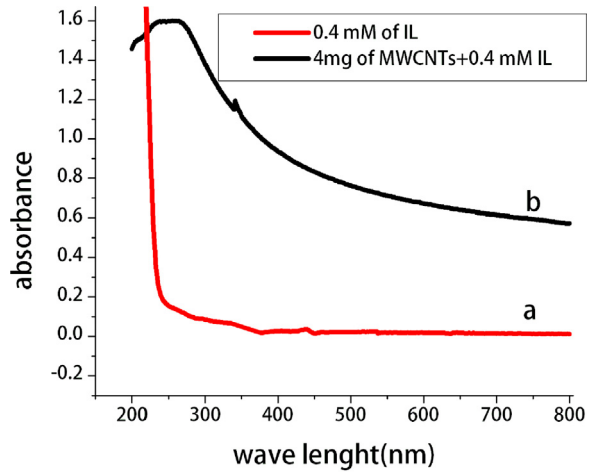

Fig. 5. UV–vis spectra of MWCNT suspensions (a) 0.4 mM of 1-methyl-3-octadecylimidazolium bromide aqueous solution and (b) 0.004 g MWCNTs dispersed in 10 ml of 0.4 mM of 1-methyl-3-octadecylimidazolium bromide aqueous solution.

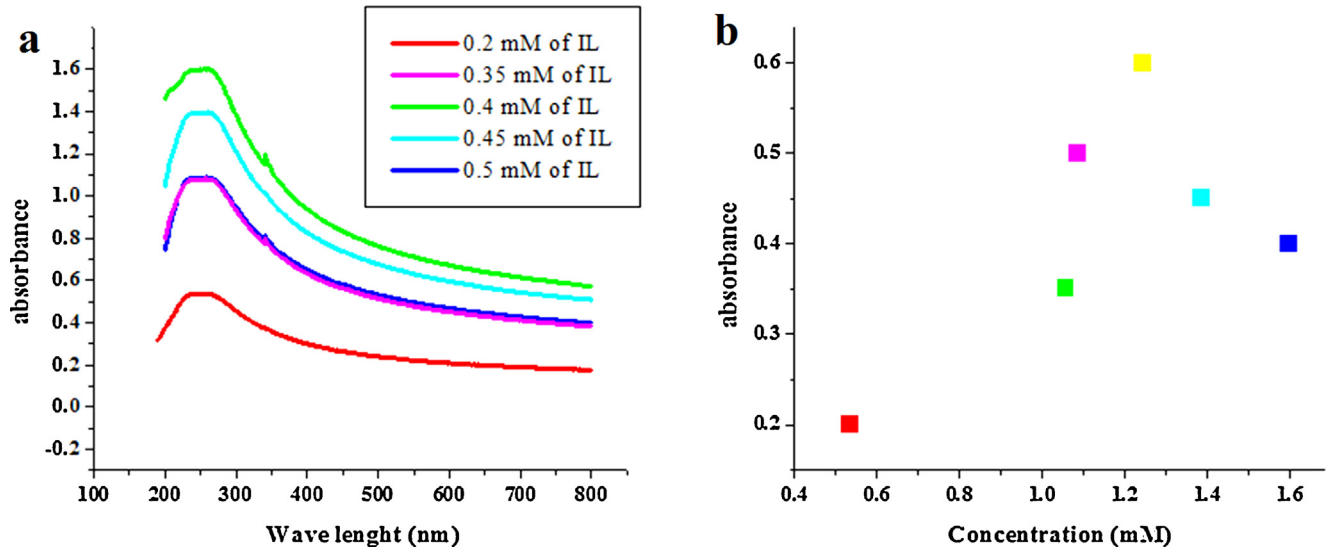

Fig. 6. (a) UV–vis spectra of aqueous MWCNT suspension with different concentration of 1-methyl-3-octadecylimidazolium bromide, (b) absorption of MWCNTs dispersions at 260 nm with increasing IL concentration (0.004 g MWCNTs dispersed in 10 ml of different concentration of [C18C1im]Br in aqueous solutions).

where $F(t)$ is sedimentation factor, which can be used to characterized the sedimentation behavior of a given dispersion [35]. Fig. 7b illustrated the variation of sedimentation function with centrifugation time. As it can be seen in Fig. 7b, the sedimentation function is decreased by raise of the centrifugation time. When a short time ultrasonication (10 min) were used for preparing a well dispersed CNTs suspension, it clearly indicated that cannot damage the structure (shortening or cutting) of CNTs [35,46], which is strongly desired in preparation of well dispersed CNTs for using in supercapacitors.

The zeta potential measurement is a common means to evaluate the stability of colloidal particles in aqueous solutions, this important parameter can visually reflect the surface charge and the magnitude of electrostatic interactions [39]. When the concentration of 1-methyl-3-octadecyleimidazolium bromide is only 0.4 mM, zeta-potential for the surface of MWCNTs is about 60 mV, which can be attributed to the tight adsorption of 1-methyl-3-octadecylimidazolium bromide on the surface of MWCNTs. The large average amount of zeta potential for dispersed CNTs in prepared suspension (60 mV), trustworthy confirmed their stability against aging [25]. Based on these results we claim that the stability of the suspension was achieved by electrostatic repulsion. Therefore long hydrophobic chain and imidazole ring head group make [C18C1im]Br as a suitable dispersing agent.

In this paper, the interaction between MWCNTs and 1-methyl-3-octadecylimidazolium bromide were studied with the FT-IR spectra. The FT-IR spectra of [C18C1im] Br, which were compared to [C18C1im] Br–stabilized MWCNTs dispersion are shown in Fig. 8a and b, respectively. The peak shifts defined the charge transfer between [C18C1im] Br and MWCNTs [25,33]. The bands in 2916 and 2851 cm^{-1} are attributed to asymmetric and symmetric vibration of methylene groups $(CH_2)_n$ of [C18C1im] Br, respectively. Because

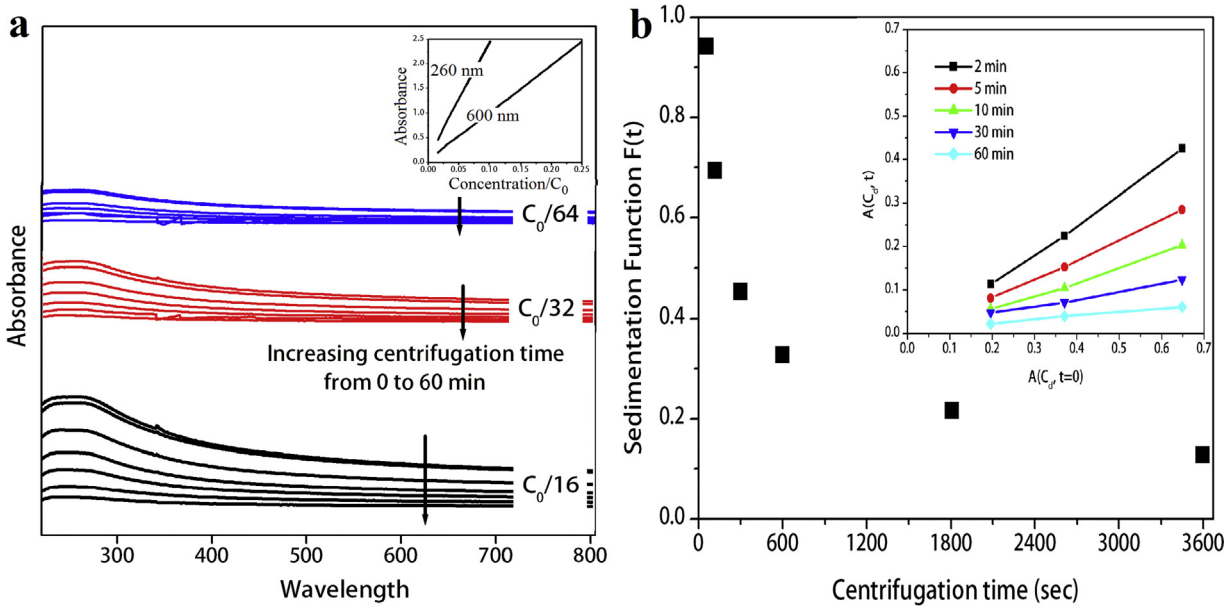

Fig. 7. (a) UV–vis spectra of diluted [C18C1im]Br stabilized MWCNT suspension (C_0/16, C_0/32, and C_0/64) and corresponding centrifuged supernatants. The inset shows the variation of the absorbance at 260 and 600 nm vs. the CNT concentration of the series dispersions without centrifugation, (b) sedimentation function of 1-metyl-3-octadecylimidazolium bromide stabilized CNTs suspensions. The inset represents the plot of $A(C_d, t)$ vs. $A(C_d, t=0)$ at 600 nm.

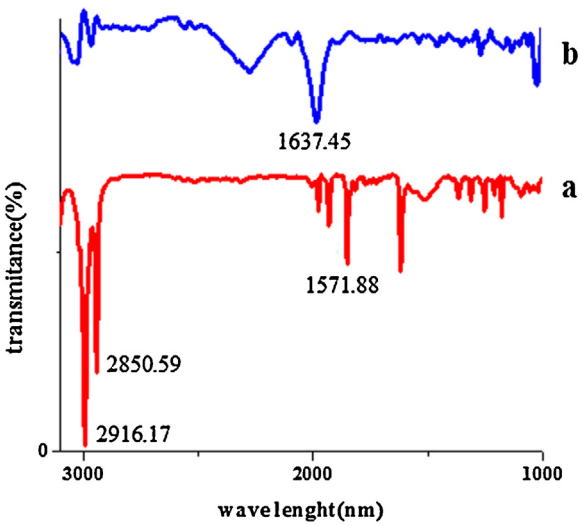

Fig. 8. FT-IR spectra of (a) 1-methyl-3-octadecylimidazolium bromide, comparing with (b) [C18C1im] Br-stabilized MWCNT dispersion.

of the hydrophobic interaction between MWCNTs and hydrocarbon chains of 1-methyl-3-octadecylimidazolium bromide, the up-shift of bands can be seen in the spectra of MWCNTs and IL mixture [33]. The bending vibration of N-C in IL at 1571.88 shows an up shift in mixture. All the peak shifts demonstrated that 1-methyl-3-octadecylimidazolium bromide can tightly adsorb on the surface of MWCNTs.

According to the UV–vis, FT-IR, and zeta-potential results, we can claim that when 1-methyl-3-octadecylimidazolium bromide is added into aqueous solution, which contains CNT bundles, [C18C1im] Br molecules can be adsorbed superiorly on the MWCNT side due to hydrophilic interaction between long chains of [C18C1im] Br and graphitic unit of MWCNTs, so it can be stabilize a CNT dispersion by columbic force between encapsulate CNTs [32].

3.2. Anodized aluminum oxide template

Fig. 9a and b shows the SEM images of the surface morphology and cross-sectional views of AAO template after two-step anodizing and pores widening treatment. We can see the straight parallel pores, perpendicular to the AAO template surface.

For both SEM images in Fig. 9, the EDX spectra confined the existence of Aluminum, oxygen, and Au (as conducting layer sputtered on the one side of the AAO templates) in the template, that referred to formation a periodic hexagonal close-packed membrane which is called AAO template (Fig. 9c).

Fig. 10a and b illustrates the SEM images of the surface and cross-sectional views of the AAO template after electrodeposition of Ni in the bottom of pores. The EDX data analysis of c and d areas which remarked in Fig. 10b were shown in Fig. 10c and d, respectively. The EDX results are trustworthy evidence that a small amount of Ni nano particles were uniformly electrodeposited at the bottom of the pores in the AAO template, which could play an important role in deposition of CNTs in the nanochannels of AAO template.

Fig. 11a illustrates the arrangement of well dispersed CNTs on the AAO template after applying an external field. As it can be seen, the porous structure of AAO template and the superior ability of [C18C1im] Br in dispersing CNTs resulted in a unique structure of CNT based electrode (without any bundles of CNTs on the upper

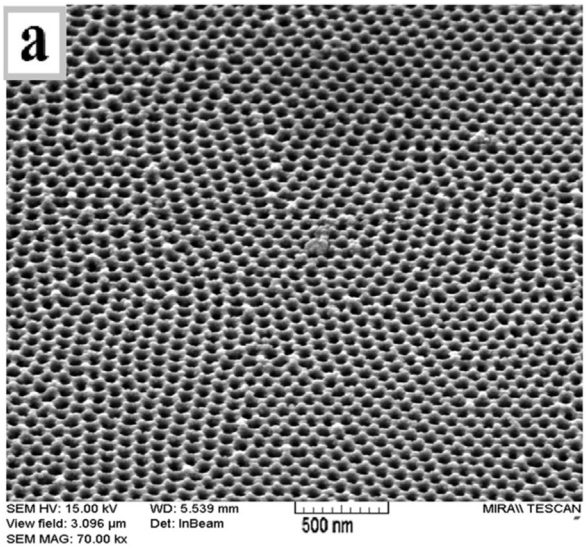

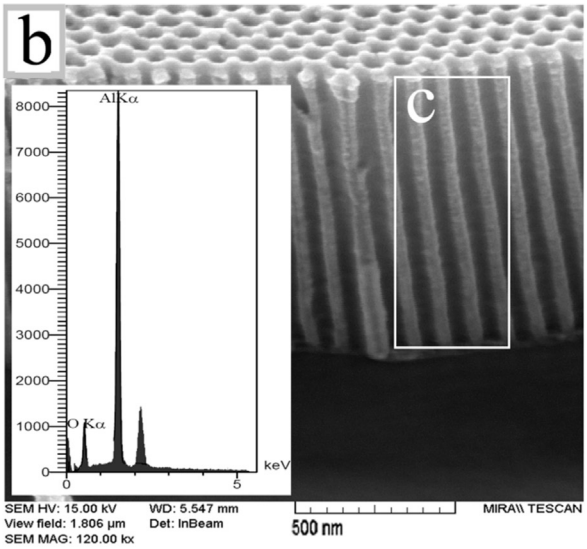

c

Quantitative Results

Element	Line	Int	Error	K	Kr	W%	A%	ZAF
O	Ka	135.8	15.4255	0.1806	0.1105	35.11	47.71	0.3148
Al	Ka	2188.8	61.9221	0.8194	0.5013	64.89	52.29	0.7725
				1.0000	0.6118	100.00	100.00	

Fig. 9. SEM images of (a) plane, (b) cross-sectional view of pore structures of anodized aluminum oxide (AAO) template. Inset shows the EDX spectrum obtained from region which remarked with c, and (c) is its EDX analysis.

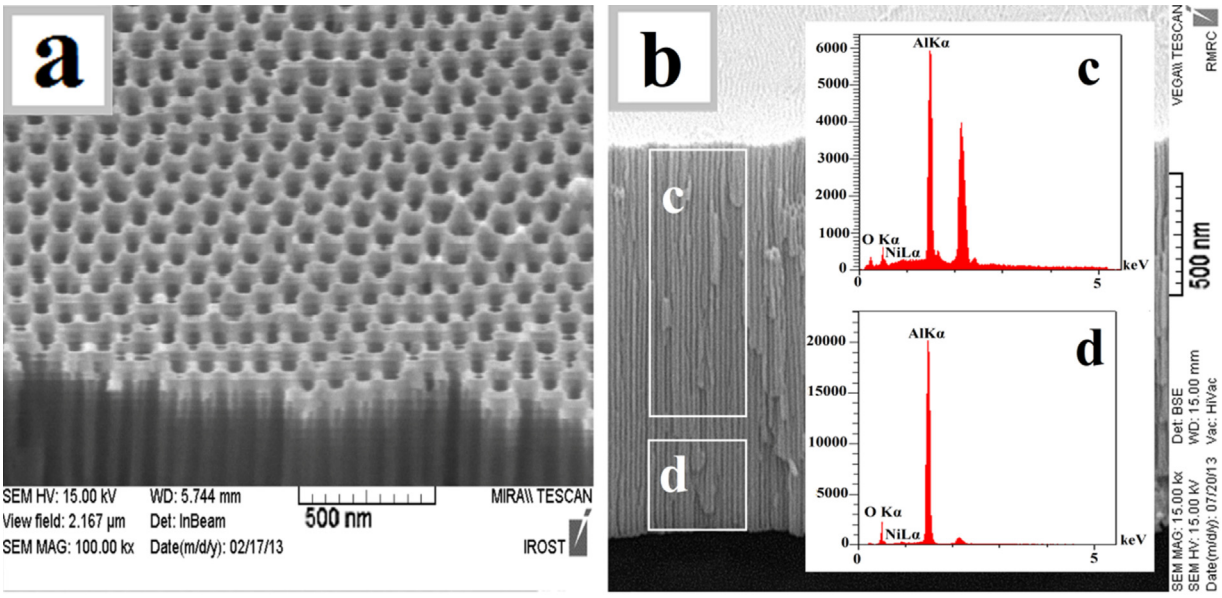

c

Quantitative Results

Element	Line	Int	Error	K	Kr	W%	A%	ZAF
O	Ka	44.9	1.0933	0.1571	0.1144	28.81	40.56	0.3970
Al	Ka	687.0	70.384	0.8429	0.6136	71.19	59.44	0.8619
Ni	Ka	0.0	0.0000	0.0000	0.0000	0.00	0.00	0.8387
				1.0000	0.7280	100.00	100.00	

d

Quantitative Results

Element	Line	Int	Error	K	Kr	W%	A%	ZAF
O	Ka	262.0	9.6284	0.2026	0.1410	33.81	46.31	0.4171
Al	Ka	2935.6	10.5270	0.7954	0.5538	66.02	53.62	0.8388
Ni	Ka	1.0	1.3750	0.0020	0.0014	0.17	0.06	0.8340
				1.0000	0.6962	100.00	100.00	

Fig. 10. SEM images of (a) surface morphology, (b) cross-sectional images of pore structures of AAO template, after Ni nanoparticles deposition, respectively. Inset shows the EDX spectrum obtained from regions which remarked with c and d, (c) and (d) are the EDX quantitative results of remarked regions in Fig. 10b.

surface of the template) which can grantee a good wetability of electrode when it used in EDLCs. Fig. 11a represents the cross sectional view of aligned CNTs which fabricated in the nanopores of AAO template. In compare with the cross sectional view of prepared AAO template before deposition of CNTs (see Fig. 9c), it can clearly seen that the nanochannels of AAO template have been filled with CNTs during the EPD process. The inset is a high magnification image of CNTs which have been deposited in the pores of AAO template. Fig. 11b illustrates EDX analysis of the region which was shown in the inset of Fig. 11a. It is evident that the material consists of C, Al, O, Au, and Ni elements. The presence of Au and Ni elements is attributed to the AAO template coated with an Au layer and being conductive with Ni nanoparticles which have been deposited in the bottom of AAO pores. According to the results, the EPD of well dispersed CNTs on the AAO nanopores filter, leads to alignment of CNTs in the pores of AAO template.

Based on the mechanism of growing nano-particles in the pores of AAO template, we suggest that the junction between the electrode surface and the bottom edge of the template pore serves as a preferential site for the deposition of individual CNTs, because the inner walls of the nanochannels have surface adsorption energy [47].

Based on our experimental results, structure of deposited film tightly depends on deposition duration and applied voltage, so we studied the effect of these parameters on deposition of [C18C1im] Br-stabilized MWCNT dispersion, which are resulted that the best time and voltage are 1 min and 100 V, respectively.

3.3. Electrochemical tests

The cyclic voltammograms (CVs) obtained from electrodes which prepared by electrophoretic deposition of MWCNT-[C18C1im] Br on porous AAO template in 1.0 M Na_2SO_4 at different scan rates are shown in Fig. 12a. The CV curves present regular shapes at relatively high scan rate (100 mV s^{-1}), indicating well-developed capacitive properties. The electrode which prepared by EPD exhibits almost mirror voltagrams with respect to the zero-current line, except for the small peaks at +0.41 and −0.24 V,

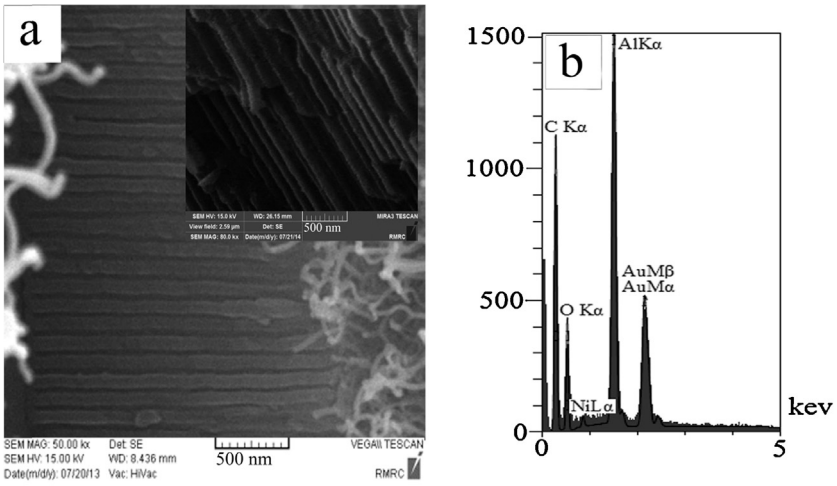

c

Quantitative Results

Element	Line	Int	Error	K	Kr	W%	A%	ZAF
C	Ka	231.1	31.6057	0.5226	0.2239	57.13	76.11	0.3918
O	Ka	73.8	31.6057	0.0832	0.0356	16.31	16.31	0.2184
Al	Ka	477.4	7.9359	0.1885	0.0807	10.49	6.22	0.7693
Ni	Ka	1.7	0.5024	0.0051	0.0022	0.26	0.07	0.8318
Au	La	4.6	0.5024	0.2006	0.0859	15.80	1.28	0.5439
				1.0000	0.4284	100.0		

Fig. 11. (a) SEM micrographs of CNTs deposited in an anodic aluminum oxide template by EPD from suspension of 0.004 g CNTs dispersed in 0.4 mM [C18C1im]Br, at 100 V cm^{-1} for 1 min. *Inset*: Cross sectional view of deposited CNTs in AAO nanochannels (b) the EDX spectrum obtained from region which shown in the inset of Image 11a, and (c) corresponding EDX results.

attributable to the redox reactions caused by the dispersant agents which were adsorbed on the surface of MWCNTs [48]. At the scan rate of 20 mV s^{-1}, capacitance of the VA-CNT electrode was found to be 51 Fgr^{-1}. As illustrated in Fig. 12b, the capacitance of resultant electrode decreased upon the scan rates increased. To investigate the performance of prepared VA-CNT electrodes, potential-time profiles of individual electrodes vs. Ag/AgCl at the constant current density of 1.25 Agr^{-1} and cut off voltages for charging-discharging of −1.2 to 0.8 V in 1.0 M Na_2SO_4 solution, were presented.

As shown in Fig. 13a, the chronopotentiogram of the prepared VA-CNT electrodes indicates a good linear variation of potential versus time, which is typical characteristic of an ideal capacitor [49]. According to Fig. 13b, the specific capacitance of resultant electrodes slightly decreases from 40 to 27 Fgr^{-1}, with the increase of discharge current density from 1.25 to 2.5 Agr^{-1}. So there is drop of the specific capacitance with increasing the discharge current density. Fig. 13c illustrates the cyclic durability of prepared VA-CNT electrodes in 1000 cycles at a discharge current density of

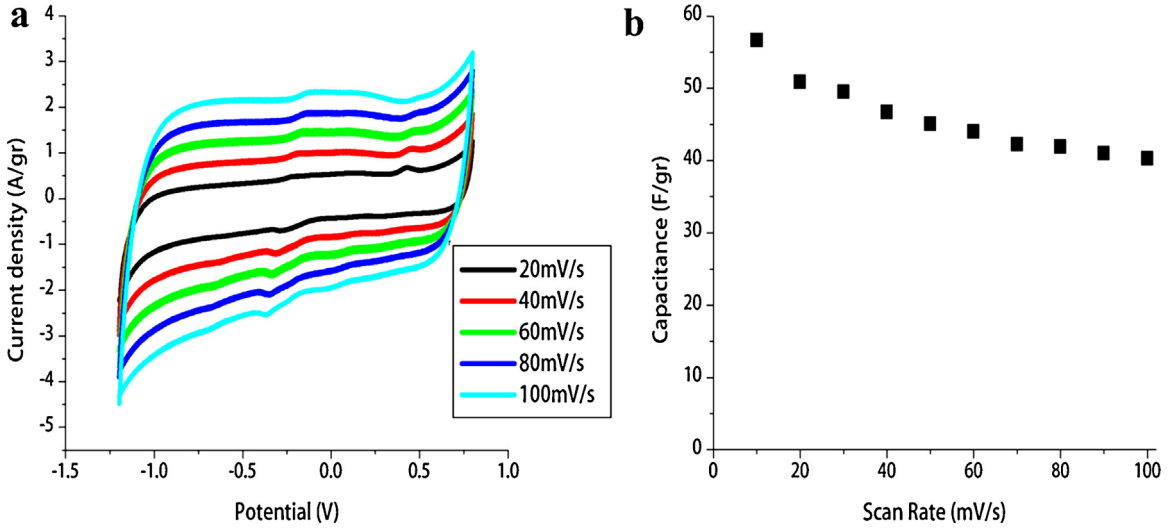

Fig. 12. (a) CVs obtained from a VA-CNT electrode in 1.0 M Na_2SO_4 at the scan rate increasing from 10 to 100 mV s^{-1}, and (b) shows the variation of capacitance with increasing the scan rate.

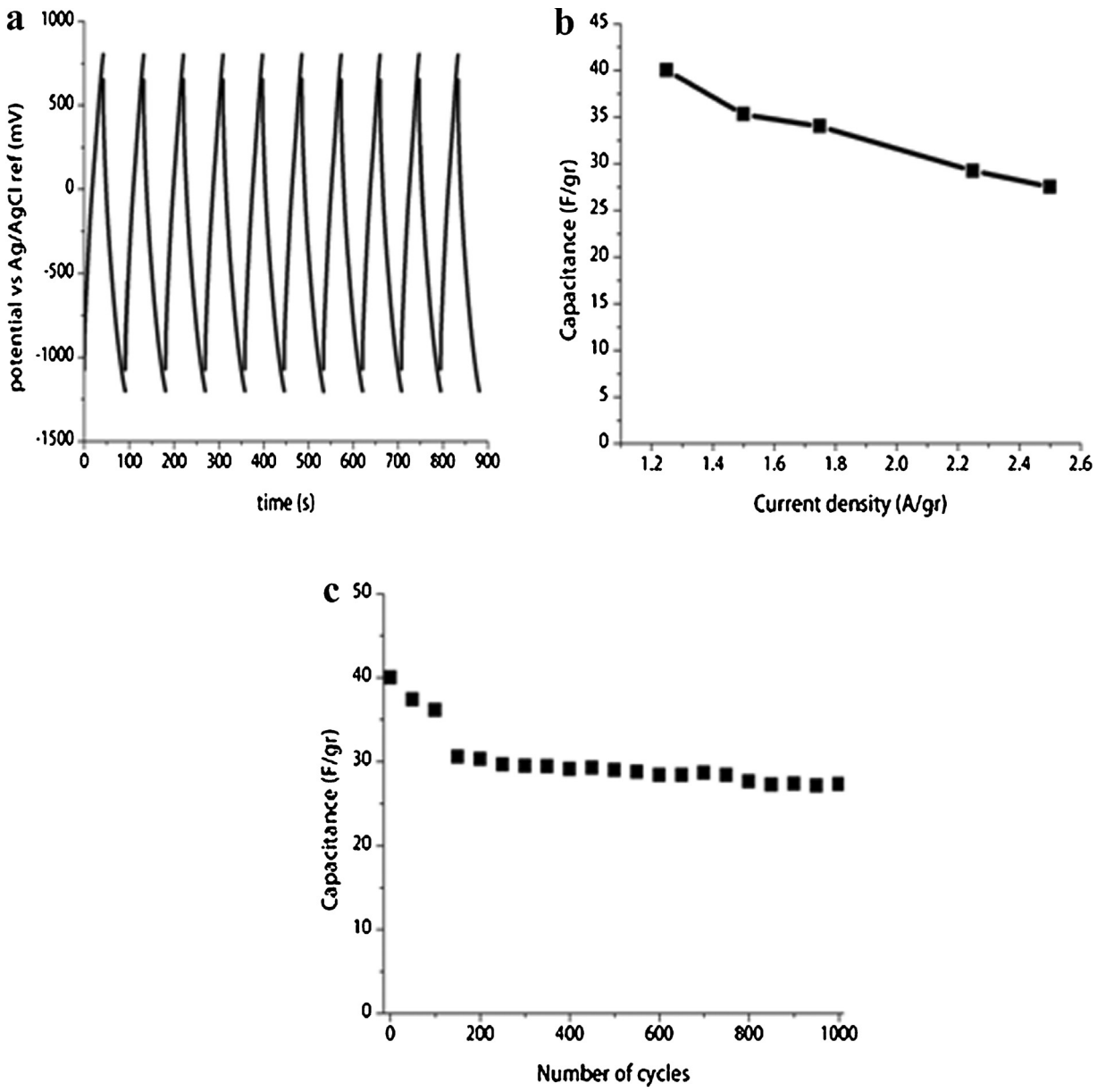

Fig. 13. (a) Constant current charge/discharge curves for VA-CNT electrode measured at 1.25 Agr^{-1} in 1.0 M Na_2SO_4 solution, between −1200 and 400 mV, and (b) The ratio of changing specific capacitance values of prepared electrode as a function of discharge current densities and (c) Capacitance retention ratio of resultant electrode as a function of cycle number.

1.25 Agr^{-1}, this curves clearly shown that the resulting electrodes retained a capacitive over 70% of the first cycle [50–52].

4. Conclusion

We have developed an easy method to fabricate well dispersed CNTs with aid of small amount of 1-methyl-3-octadecylimidazolium bromide by EPD in AAO substrate, where synthesized by two-step anodization of Aluminum at 5 °C. The AAO templates were became conductive by electrochemical deposition of Ni nanoparticles in the bottom of pores. This method enables us to obtain vertically aligned CNTs. We expect that this method can be directly applied to fabrication of a VACNT based electrode for the CNT-based EDLCs. Etching of the template gives us CNTs with very similar dimensions. We have developed a new generation of VA-CNT with 50 Fgr^{-1} specific capacitance. It seems to be very useful to a model study for many CNT-based applications.

Acknowledgements

We are grateful for financial support from Iran National Science Foundation (INSF), Iran (Grant No. 93/36575).

References

[1] S. Iijima, Helical microtubules of graphitic carbon, Nature 345 (1991) 56–58, http://dx.doi.org/10.1038/354056a0.
[2] J.M. Bonard, J.P. Salvetat, T. Stöckli, L. Forró, A. Châtelain, Field emission from carbon nanotubes: perspectives for applications and clues to the emission mechanism, Appl. Phys. A 69 (1999) 245–254, http://dx.doi.org/10.1007/s003399900113.
[3] W. Zhu, C. Bower, O. Zhou, G. Kochanski, S. Jin, Large current density from carbon nanotube field emitters, Appl. Phys. Lett. 75 (6) (1999) 873–875, http://dx.doi.org/10.1063/1.124541.
[4] A.C. Dillon, K.M. Jones, T.A. Bekkedahl, C.H. Kiang, D.S. Bethune, M.J. Heben, Storage of hydrogen in single-walled carbon nanotubes, Nature 386 (1997) 377–379, http://dx.doi.org/10.1038/386377a0.

[5] C. Liu, Y.Y. Fan, M. Liu, H.T. Cong, H.M. Cheng, M.S. Dresselhaus, Hydrogen storage in single-walled carbon nanotubes at room temperature, Science 286 (5442) (1999) 1127–1129, http://dx.doi.org/10.1126/science.286.5442.1127.
[6] E. Frackowiak, S. Gautier, H. Gaucher, S. Bonnamy, F. Beguin, Electrochemical storage of lithium in multiwalled carbon nanotubes, Carbon 37 (1) (1999) 61–69, http://dx.doi.org/10.1016/S0008-6223(98)00187-0.
[7] C. Niu, E.K. Sichel, R. Hoch, D. Moy, H. Tennent, High power electrochemical capacitors based on carbon nanotube electrodes, Appl. Phys. Lett. 70 (11) (1997) 1480–1482, http://dx.doi.org/10.1063/1.118568.
[8] C.Y. Liu, A.J. Bard, F. Wudl, I. Weitz, J.R. Heath, Electrochemical characterization of films of single-walled carbon nanotubes and their possible application in supercapacitors, Electrochem. Solid-State Lett. 2 (11) (1999) 577–578, http://dx.doi.org/10.1149/1.1390910.
[9] J.J. Davis, R.J. Coles, H. Allen, O. Hill, Protein electrochemistry at carbon nanotube electrodes, J. Electroanal. Chem. 440 (1–2) (1997) 279–282, http://dx.doi.org/10.1016/S0022-0728(97)80067-8.
[10] R.H. Baughman, C. Cui, A.A. Zakhidov, Z. Iqbal, J.N. Barisci, G.M. Spinks, et al., Carbon nanotube actuators, Science 284 (5418) (1999) 1340–1344, http://dx.doi.org/10.1126/science.284.5418.1340.
[11] S.K. Kim, H. Lee, H. Tanaka, P.S. Weiss, Vertical alignment of single-walled carbon nanotube films formed by electrophoretic deposition, Langmuir 24 (22) (2008) 12936–12942, http://dx.doi.org/10.1021/la802266y.
[12] H.J. Ahn, J.I. Sohn, Y.S. Kim, H.S. Shim, W.B. Kim, T.Y. Seong, Electrochemical capacitors fabricated with carbon nanotubes grown within the pores of anodized aluminum oxide templates, Electrochem. Commun. 8 (4) (2006) 513–516, http://dx.doi.org/10.1016/j.elecom.2006.01.018.
[13] S. Wen, S.I. Mho, I.H. Yeo, Improved electrochemical capacitive characteristics of the carbon nanotubes grown on the alumina templates with high pore density, J. Power Sources 163 (1) (2006) 304–308, http://dx.doi.org/10.1016/j.jpowsour.2006.01.064.
[14] K. Iakoubovskii, Techniques of aligning carbon nanotubes, Cent. Eur. J. Phys. 7 (4) (2009) 645–653, http://dx.doi.org/10.2478/s11534-009-0072-2.
[15] M. Chhowalla, K.B.K. Teo, C. Ducati, N.L. Rupesinghe, G.A.J. Amaratunga, FerrariAC, et al., Growth process conditions of vertically aligned carbon nanotubes using plasma enhanced chemical vapor deposition, J. Appl. Phys. 90 (10) (2001) 5308–5317, http://dx.doi.org/10.1063/1.1410322.
[16] H. Zhang, G. Cao, Y. Yang, Z. Gu, Capacitive performance of an ultralong aligned carbon nanotube electrode in an ionic liquid at 60 °C, Carbon 46 (1) (2008) 30–34, http://dx.doi.org/10.1016/j.carbon.2007.10.023.
[17] M. Lahav, T. Sehayek, A. Vaskevich, I. Rubinstein, Nanoparticle nanotubes, Angew. Chem. 115 (2003) 5734–5737, http://dx.doi.org/10.1002/ange.200352216.
[18] A.R. Boccaccini, C. Kaya, M.S.P. Shaffer, Electrophoretic deposition of carbon nanotubes (CNTs) and CNT/nanoparticle composites, in: J.H. Dickerson, A.R. Boccaccini (Eds.), Electrophoretic Deposition of Nanomaterials, Springer, New York, 2012, pp. 157–179.
[19] L. Jin, C. Bower, O. Zhou, Alignment of carbon nanotubes in a polymer matrix by mechanical stretching, Appl. Phys. Lett. 73 (1998) 1197–1199, http://dx.doi.org/10.1063/1.122125.
[20] N. Bendiab, R. Almairac, J.L. Sauvajol, S. Rols, E. Elkaim, Orientation of single-walled carbon nanotubes by uniaxial pressure, J. Appl. Phys. 93 (3) (2003) 1769–1773, http://dx.doi.org/10.1063/1.1534905.
[21] M.D. Haslam, B. Raeymaekers, Aligning carbon nanotubes using bulk acoustic waves to reinforce polymer composites, Composites Part B 60 (2014) 91–97, http://dx.doi.org/10.1016/j.compositesb.2013.12.027.
[22] W.A. de Heer, J.M. Bonard, K. Fauth, A. Chatelain, L. Forro, D. Ugarte, Electron field emitters based on carbon nanotube films, Adv. Mater. 9 (1) (1997) 87–89, http://dx.doi.org/10.1002/adma.19970090122.
[23] S. Zhang, K.K. Koziol, I.A. Kinloch, A.H. Windle, Macroscopic fibers of well-aligned carbon nanotubes by wet spinning, Small 4 (8) (2008) 1217–1222, http://dx.doi.org/10.1002/smll.200700998.
[24] A.R. Boccaccini, J. Cho, J.A. Roether, B.J.C. Thomas, E.J. Minay, M.S.P. Shaffer, Electrophoretic deposition of carbon nanotubes, Carbon 44 (15) (2006) 3149–3160, http://dx.doi.org/10.1016/j.carbon.2006.06.021.
[25] F. Lu, S. Zhang, L. Zheng, Dispersion of multi-walled carbon nanotubes (MWCNTs) by ionic liquid-based phosphonium surfactants in aqueous solution, J. Mol. Liq. 173 (2012) 42–44, http://dx.doi.org/10.1016/j.molliq.2012.06.012.
[26] M. López-Pastor, A. Domínguez-Vidal, M.J. Ayora-Cañada, B.M. Simonet, B. Lendl, M. Valcárcel, Separation of single-walled carbon nanotubes by use of ionic liquid-aided capillary electrophoresis, Anal. Chem. 80 (8) (2008) 2672–2679, http://dx.doi.org/10.1021/ac701788r.
[27] A. Thess, R. Lee, P. Nikolaev, H. Dai, P. Petit, J. Robert, et al., Crystalline ropes of metallic carbon nanotubes, Science 273 (5274) (1996) 483–487, http://dx.doi.org/10.1126/science.273.5274.483.
[28] J. Wang, H. Chu, Y. Li, Why single-walled carbon nanotubes can be dispersed in imidazolium-based ionic liquids, ACS Nano 2 (12) (2008) 2540–2546, http://dx.doi.org/10.1021/nn800510g.
[29] T. Fukushima, A. Kosaka, Y. Ishimura, YamamotoT, T. Takigawa, N. Ishii, et al., Molecular ordering of organic molten salts triggered by single-walled carbon nanotubes, Science 300 (5628) (2003) 2072–2074, http://dx.doi.org/10.1126/science.1082289.
[30] A. Di Crescenzo, D. Demurtas, A. Renzetti, G. Siani, P. De Maria, M. Meneghetti, et al., Disaggregation of single-walled carbon nanotubes (SWNTs) promoted by the ionic liquid-based surfactant 1-hexadecyl-3-vinylimidazolium bromide in aqueous solution, Soft Matter 5 (2009) 62–66, http://dx.doi.org/10.1039/B812022F.
[31] N. Kocharova, T. Ääritalo, J. Leiro, J. Kankare, J. Lukkari, Aqueous dispersion, surface thiolation, and direct self-assembly of carbon nanotubes on gold, Langmuir 23 (6) (2007) 3363–3371, http://dx.doi.org/10.1021/la0631522.
[32] Y. Liu, L. Yu, S. Zhang, J. Yuan, L. Shi, L. Zheng, Dispersion of multiwalled carbon nanotubes by ionic liquid-type Gemini imidazolium surfactants in aqueous solution, Colloids Surf. A 359 (1–3) (2010) 66–70, http://dx.doi.org/10.1016/j.colsurfa.2010.01.065.
[33] H. Gao, S. Zhang, D. Huang, L. Zheng, Dispersion of multi-wall carbon nanotubes by an ionic liquid-based polyether in aqueous solution, Colloid. Polym. Sci. 290 (8) (2012) 757–762, http://dx.doi.org/10.1007/s00396-012-2619-9.
[34] S. Attal, R. Thiruvengadathan, O. Regev, Determination of the concentration of single-walled carbon nanotubes in aqueous dispersions using UV–visible absorption spectroscopy, Anal. Chem. 78 (2006) 8098–8104, http://dx.doi.org/10.1021/ac060990s.
[35] T. Liu, S. Luo, Z. Xiao, C. Zhang, B. Wang, Preparative ultracentrifuge method for characterization of carbon nanotube dispersions, J. Phys. Chem. C 112 (2008) 19193–19202, http://dx.doi.org/10.1021/jp804720j.
[36] A.I. López-Lorente, B.M. Simonet, M. Valcárcel, Raman spectroscopic characterization of single walled carbon nanotubes: influence of the sample aggregation state, Analyst 139 (2014) 290–298, http://dx.doi.org/10.1039/c3an00642e.
[37] D. Yoon, J.B. Choi, C.S. Han, Y.J. Kim, S. Baik, The quantitative characterization of the dispersion state of single-walled carbon nanotubes using Raman spectroscopy and atomic force microscopy, Carbon 46 (2008) 1530–1534, http://dx.doi.org/10.1016/j.carbon.2008.06.046.
[38] A.M. Md Jani, D. Losic, N.H. Voelcker, Nanoporous anodic aluminium oxide: advances in surface engineering and emerging applications, Prog. Mater. Sci. 58 (5) (2013) 636–704, http://dx.doi.org/10.1016/j.pmatsci.2013.01.002.
[39] M.R. Mohammadi, F. Ordikhani, D.J. Fray, F. Khomamizadeh, Template-based growth of titanium dioxide nanorods by a particulate sol-electrophoretic deposition process, Particuology 9 (2) (2011) 161–169, http://dx.doi.org/10.1016/j.partic.2010.07.026.
[40] C.G. Jin, W.F. Liu, C. Jia, X.Q. Xiang, W.L. Cai, L.Z. Yao, X.G. Li, High-filling, large-area Ni nanowire arrays and the magnetic properties, J. Cryst. Growth 258 (3–4) (2003) 337–341, http://dx.doi.org/10.1016/S0022-0248(03)01542-2.
[41] G. Meng, A. Cao, J.Y. Cheng, A. Vijayaraghavan, Y.J. Jung, M. Shima, P.M. Ajayan, Ordered Ni nanowire tip arrays sticking out of the anodic aluminum oxide template, J. Appl. Phys. 97 (2005) 064303, http://dx.doi.org/10.1063/1.1846942.
[42] G.D. Sulka, A. Brzózka, L. Zaraska, M. Jaskuła, Through-hole membranes of nanoporous alumina formed by anodizing in oxalic acid and their applications in fabrication of nanowire arrays, Electrochim. Acta 55 (14) (2010) 4368–4376, http://dx.doi.org/10.1016/j.electacta.2010.01.048.
[43] W. Hu, L. Yuan, Z. Chen, D. Gong, K. Saito, Fabrication and characterization of vertically aligned carbon nanotubes on silicon substrates using porous alumina nanotemplates, J. Nanosci. Nanotechnol. 2 (2) (2002) 203–207, http://dx.doi.org/10.1166/jnn.2002.104.
[44] K. Nielsch, F. Müller, A.P. Li, U. Gösele, Uniform nickel deposition into ordered alumina pores by pulsed electrodeposition, Adv. Mater. 12 (2000) 582–586, http://dx.doi.org/10.1002/(SICI)1521-4095(200004)12:8<582::AID-ADMA582>3.0.CO;2-3.
[45] A. Cortés, G. Riveros, J.L. Palma, J.C. Denardin, R.E. Marotti, E.A. Dalchiele, H. Gómez, Single-crystal growth of nickel nanowires: influence of deposition conditions on structural and magnetic properties, J. Nanosci. Nanotechnol. 9 (3) (2009) 1992–2000, http://dx.doi.org/10.1166/jnn.2009.374.
[46] Q. Wang, Y. Han, Y. Wang, Y. Qin, Z.X. Guo, Effect of surfactant structure on the stability of carbon nanotubes in aqueous solution, J. Phys. Chem. B 112 (2008) 7227–7233, http://dx.doi.org/10.1021/jp711816c.
[47] X. Li, Y. Wang, G. Song, Z. Peng, Y. Yu, X. She, J. Li, Synthesis and growth mechanism of Ni nanotubes and nanowires, Nanoscale Res. Lett. 4 (2009) 1015–1020, http://dx.doi.org/10.1007/s11671-009-9348-0.
[48] M. Opallo, A. Lesniewski, A review on electrodes modified with ionic liquids, J. Electroanal. Chem. 656 (1–2) (2011) 2–16, http://dx.doi.org/10.1016/j.jelechem.2011.01.008.
[49] A. Zolfaghari, F. Ataherian, M. Ghaemi, A. Gholami, Capacitive behavior of nanostructured MnO_2 prepared by sonochemistry method, Electrochim. Acta 52 (8) (2007) 2806–2814, http://dx.doi.org/10.1016/j.electacta.2006.10.035.
[50] J.S. Lauret, C. Voisin, G. Cassabois, C. Delalande, Ph. Roussignol, O. Jost, L. Capes, Ultrafast carrier dynamics in single-wall carbon nanotubes, Phys. Rev. Lett. 90 (2003) 057404, http://dx.doi.org/10.1103/PhysRevLett.90.057404.
[51] Q. Chen, K. Xue, W. Shen, F. Tao, S. Yin, W. Xu, Fabrication and electrochemical properties of carbon nanotube array electrode for supercapacitors, Electrochim. Acta 49 (24) (2004) 4157–4161, http://dx.doi.org/10.1016/j.electacta.2004.04.010.
[52] N. Handa, T. Sugimoto, M. Yamagata, M. Kikuta, M. Kono, M. Ishikawa, A neat ionic liquid electrolyte based on FSI anion for electric double layer capacitor, J. Power Sources 185 (2) (2008) 1585–1588, http://dx.doi.org/10.1016/j.jpowsour.2008.08.086.